MEGA JOURNAL OF CASE REPORTS

Research Article

Compiled Date: January 20, 2023

Activation of Human Fibroblasts by Pancreatic Cancer Cell Lines

Dina Safina[1]*, Nataliya Lunina[1], Marina Roschina[1], Oksana Staeglasova[1], Andrey Kazakov[2], Vladimir Demkin[2], Ilya Demidyuk[1] and Sergey Kostrov[1]

[1]Department of Molecular-Genetic Basis of Biotechnology and Protein Engineering, National Research Centre "Kurchatov Institute", Russia

[2]Center for Cellular and Genetic Technologies, National Research Centre "Kurchatov Institute", Russia

***Corresponding author**: Dina Safina, Department of Molecular-Genetic Basis of Biotechnology and Protein Engineering, National Research Centre "Kurchatov Institute", Moscow 123182, Russia, Tel: 79104583318; E-mail: nauruz@mail.ru

Abstract

The efficiency of activation of normal human dermal fibroblasts by human pancreatic adenocarcinoma cell lines was comparatively studied. The effect of the obtained cancer-associated fibroblasts (CAFs) on the cancer cell migration potential was studied *in vitro* and at the organism level in a zebrafish embryo xenotransplantation model. The data obtained indicate several stages of changes in the functional state of fibroblasts exposed to cancer cells, which are likely mediated by different mechanisms and aimed at different biological endpoints. For instance, paracrine factors released by cancer cells rapidly increase the migration rate of fibroblasts, which may recruit stromal fibroblasts to growing cancer. At the same time, direct contact of fibroblasts with cancer cells modifies their morphological status and induces cancer-dependent changes in several marker genes. Thus, cell interaction with cancer cells involves additional molecular mechanisms not induced by paracrine factors. Yet, despite specific activation signs after co-cultivation with cancer cells, fibroblasts failed to modulate the migration efficiency of cancer cells in the zebrafish *in vivo* model.

Keywords: Human pancreatic adenocarcinoma; Cell migration; Fibroblast activation; Cancer-associated fibroblasts; Zebrafish model

Introduction

Metastasis is among the most sinister and obscure processes. At the same time, only certain cancer types include special malignant cells with the properties required to generate metastases. In most cases, numerous and structurally complex factors mediating cancer cell interaction with their stromal environment can trigger the metastatic cascade **[1-3].** Apparently, Cancer-Associated Fibroblasts (CAFs) are the key element of the stromal environment involved in the control of cancer progression and metastasis. CAFs are a special group of

fibroblasts whose properties alter after the interaction with progressing tumor cells **[4,5].** At the same time, CAFs can induce tumor progression including metastasis. The mechanisms underlying the prometastatic activity of CAFs include their impact on different elements of the metastatic cascade. Amongst them are induction of invasive phenotype of cancer cells through the increase in their epithelial-mesenchymal plasticity **[6-8],** structural modification of the extracellular matrix **[9]**, formation of migrating heterotypic cell clusters **[10,11],** cancer cell survival in the bloodstream **[10],** blood supply of secondary tumor nodules **[12],** etc. The close relationship between tumor and stromal cells in cancer progression **[13,14]** suggests the development of "anti-stromal" therapies **[15,16]** aimed among other things at metastasis suppression through blocking specific cell-to-cell interactions. CAFs are among the key targets for such suppression **[17,18].** Unfortunately, extremely high heterogeneity of tumor formations *in vivo* including various populations of both malignant and stromal cells makes it hardly possible to identify the role of individual processes in the overall integration network. Accordingly, studies of natural malignant processes should be complemented by the analysis of simpler experimental systems **[19,20].** Here, we comparatively studied the efficiency of activation of normal human fibroblasts by cancer cell lines *in vitro*. The effect of the obtained CAFs on the cancer cell migration potential was analyzed *in vitro* and at the organism level.

Materials and Methods

Cell cultures

The primary continuous line of dermal fibroblasts from a normal human donor, Fb(h) [21], was provided by the Laboratory of Molecular Neurogenetics and Innate Immunity, Institute of Molecular Genetics of the National Research Centre "Kurchatov Institute". Pancreatic cancer cell lines PANC-1_GFP and MIA PaCa-2_GFP stably expressing fluorescent GFP were provided by the Shemyakin-Ovchinnikov Institute of Bioorganic Chemistry of the Russian Academy of Sciences **[22].**

Generation of conditioned media

Conditioned media were obtained by inoculating 10^5 PANC-1_GFP, MIA PaCa-2_GFP, or Fb(h) cells in 2.5 ml of DMEM/F12 (1:1 v/v) (PanEco, Russia) containing 10% fetal calf serum (GE Healthcare, United States) and 0.3 mg/ml glutamine (MP Biomedicals, United States) into 6-well plates (SPL Life Sciences Co., Ltd., South Korea). Cells were cultured for three days. The conditioned medium was collected and filtered through a 0.22 µm membrane. Cells were counted in wells using a Countess II FL cell counter (Thermo Fisher Scientific, United States) after treatment with 0.25% trypsin in Hanks solution (PanEco, Moscow, Russia) and washing with PBS (PanEco, Russia).

Fibroblast culture in conditioned media

Fb(h) cells were plated at 10^5 cells/well in three replicates into 6-well plates with the standard growth medium and incubated at 37 °C under 5% CO_2. The medium was replaced after 1 day with the obtained conditioned media. The added medium volume corresponded to that obtained from 10^5 cells. When necessary, the conditioned medium was diluted with the standard growth medium.

Later on, the conditioned medium was replaced every 3 days. The Fb(h) control was incubated in the standard growth medium. Cells were cultured in conditioned media for 18-20 days. Fibroblast viability cultured in the standard and conditioned media was tested every 3 days according to the Simple ThermoFisher protocol (https://www.thermofisher.com/ru/ru/home/life-science/cell-analysis/cell-analysis-instruments/automated-cell-

counters/features.html#Simple) using Trypan Blue Dye (cat # 1450013; Bio-Rad Laboratories, United States). After 20 days of culture, the proportion of living Fb(h) cells cultured in media conditioned by PANC-1_GFP or MIA PaCa-2_GFP cells was 65±9.5%, while Fb(h) cells cultured in the medium conditioned by Fb(h) or standard medium was 94±0.6 %.

Fibroblast coculture with cancer PANC-1_GFP and MIA PaCa-2_GFP cells

Human fibroblasts and PANC-1_GFP or MIA PaCa-2_GFP cells were cocultured at 1:1 in 6-well plates with the standard growth medium at 37 °C under 5% CO_2 in triplicates. The total number of cells was 10^5 per well. Fb(h) cells grown in the standard growth medium served as control. Cells were cocultured for five days. The medium was replaced every 2 days. The viability of fibroblast co-cultured with PANC-1_GFP and MIA PaCa-2_GFP was evaluated daily after sorting out Fb(h) cells from the culture (method described below) with an MA900 Multi-Application Cell Sorter (Sony, Japan) according to the Simple ThermoFisher protocol (https://www.thermofisher.com/ru/ru/home/life-science/cell-analysis/cell-analysis-instruments/automated-cell-counters/features.html#Simple) with Trypan Blue Dye (cat # 1450013; Bio-Rad Laboratories, United States). By culture day 5, the proportion of living Fb(h) cells co-cultured with cancer cells was 94±2.9%, while that grown in the standard medium was 97.4± 0.2%.

Evaluation of cell morphological parameters

Morphological parameters of Fb(h) cells were evaluated by daily photographing cells throughout the experiment using a direct fluorescent microscope DM1000 with a GFP ET filter cube (Ex 470/40, Em 525/50) and an ICC50 HD camera (Leica Microsystems, Germany). Cells were photographed in three independent fields of vision; 25-30 cells were analyzed in each field. The photographs were processed using the QCapture Pro 6.0 software to record individual cell parameters.

Cell sorting

The population of Fb(h) cells was isolated from the mixture with cancer PANC-1_GFP or MIA PaCa-2_GFP cells using an MA900 Multi-Application Cell Sorter (Sony, Japan) following the manufacturer's instructions. Prior to sorting, the suspension was exposed to 0.25% trypsin in Hanks solution (PanEco, Russia) and washed with PBS (PanEco, Russia). Cells were counted in a Countess II FL cell counter (Thermo Fisher Scientific, United States).

RNA isolation and quantitative PCR (qPCR)

Total DNA and RNA were isolated from 10^5 cells using a commercial kit for DNA/RNA extraction from blood (Litech, Russia) according to the manufacturer's instructions. The isolated nucleic acids were eluted in 100 µl of RNase-free water and quantified by qPCR using assays for DNA (surviving/*BIRC5* gene) and RNA (ubiquitin gene, *UBC*) detection. cDNA was prepared from each sample using the High-Capacity cDNA Reverse Transcription kit (Applied Biosystems/Thermo Fisher Scientific, Waltham, MA, USA) according to the manufacturer's instructions. The final cDNA volume was 60 µl. qPCR was performed with a CFX96 amplifier (Bio-Rad Laboratories, Inc., United States) using the Taqman assays for *IL6* (Hs00 569839_m1), *PDGFRA* (Hs00998018_m1), *ACTA2* (Hs00909449_m1) (Applied Biosystems/Thermo Fisher Scientific, United States), and *UBC* (NanoDiagnostics, Russia). All assays are designed in such a way that the probe spans the exon junction and should not detect genomic DNA. This point was confirmed in special tests. The reaction mixture included the PCR buffer, 10 mM Tris HCl, pH 8.3; 8% sucrose; 50 mM KCl; 0.5% Tween 20; 3% formamide; 3.6 mM $MgCl_2$, 180 µM of each dNTP, primers, Fam- or Hex-labeled probe, 1 U of Taq DNA polymerase, and

5 µl sample. The concentrations of the Applied Biosystems oligonucleotides were 0.9 and 0.25 µM for the primers and probe, respectively; NanoDiagnostics oligonucleotides, 0.17 µM for both primers and probe. The amplification program included 1 cycle at 95 °C for 2 min; 40 cycles at 95 °C for 10 s, 60 °C for 20 s, and 70 °C for 10 s; and 1 cycle at 70 °C for 3 min. Each experiment was repeated twice and all samples were analyzed in triplicates. Average values were used in subsequent calculations. All Ct values were normalized to the DNA contents of the *BIRC5* gene and the RNA reference gene *UBC*, and the ΔCt values were calculated **[23].**

Fb(h) cell migration in vitro

Fb(h) cells (3×10^3) prestained with the lipophilic fluorochrome CM-DiI (Invitrogen Ltd, Renfrewshire Scotland) were cultured on a polycarbonate membrane with 8-µm pores in Transwell inserts (Corning Incorporated, United States) in 100 µl of the standard growth medium in three replicates. The inserts were placed into plate wells containing 600 µl of different conditioned media. After Fb(h)_CM DiI incubation for 24 and 48 h at 37 °C under 5% CO_2, the inserts were washed with PBS (PanEco, Russia) and cells on the inner membrane surface were removed with a cotton swab. Fb(h)_CM DiI cells that migrated to the outer membrane surface were counted in five independent fields on each insert using a direct fluorescent microscope DM1000 with an N2.1 filter cube (Ex 535/45, Em LP 590) and an ICC50 HD camera (Leica Microsystems, Germany).

Maintenance of zebrafish

Fish were kept in a flow-through aquarium system (Aqua Schwarz, Germany) at 28 °C. Following international standards, the light cycle was 14 h of light and 10 h of darkness. Fish were fed once a day with nauplii *Artemia salina* (Barrom, Russia) and dry food (SeraVipan, Germany). The wild type *Danio rerio* AB line was used.

Cell preparation for transplantation

PANC-1_GFP, MIA PaCa-2_GFP, and prestained Fb(h)_CM DiI cells were used for transplantation into the developing zebrafish embryo. Cells were plated at 10^5 cells per well in a 6-well plate with the standard growth medium and cultured at 37°C under 5% CO_2 for 4 days. PANC-1_GFP plus Fb(h)_CM DiI and MIA PaCa-2_GFP plus Fb(h)_CM DiI cells were cocultured at a 1:1 ratio. The cell suspension for the injection was prepared by the exposure of cells without the medium to 0.25% trypsin in Hanks solution (PanEco, Russia) and washing with PBS (PanEco, Russia). Cells were counted in a Countess II FL cell counter (Thermo Fisher Scientific, United States) and resuspended in PBS at 10^6 cells per 100 µl. In the case of cell suspensions mixed on the day of transplantation, cells in individual lines were counted and mixed 1:1 to yield 10^6 cells per 100 µl of PBS.

Transplantation of cells into zebrafish embryo

Embryos at 48 hours post-fertilization (hpf) were dechorionated and anesthetized with 0.02% Tricain (Sigma-Aldrich, United States) prior to transplantation. Anesthetized embryos were placed on an agarose pad and pressure-injection was performed into the yolk sac using a Nanoliter 2000 system (World Precision Instruments, United States) under a stereomicroscope Olympus SZ51 (Olympus, Japan). Glass capillaries (cat.# 504949 World Precision Instruments, United States) with the outer diameter of 40 µm were obtained using a Pipette Puller Model P-100 (Sutter Instrument, United States). The injection volume was about 20 nl with the calculated content of 2×10^2 cells. After injection, the embryos were incubated in water at 28 °C for 2 h after which the temperature was raised to 34 °C. Five hours post injection, the injected embryos were bioimaged to select specimens with at least 100 cells after the injection site and no cells detected in blood vessels.

Bioimaging

Bioimaging of embryos was performed using a direct fluorescent microscope DM1000 equipped with GFP ET (Ex 470/40, Em 525/50) and N2.1 (Ex 535/45, Em LP 590) cube filters and an ICC50 HD camera (Leica Microsystems, Germany) two days after xenotransplantation. The migration activity of cells was presented as the number of embryos showing cell migration from the injection site into both blood vessels and perivitelline space. The percentage of embryos showing cell migration per total number of analyzed specimens was calculated.

Statistical analysis of experimental data

The data obtained were analyzed using MS Excel 2007 (Microsoft, United States) and SigmaPlot 12.5 (Systat Software, United States). The intergroup significance was evaluated using the student's test for two independent samples. Differences were considered significant at $p < 0.05$.

Results

Markers of fibroblast activation and cell lines

Two approaches to obtain CAF *in vitro* were analyzed here. The first one involved the exposure of cultured fibroblasts to the medium conditioned by tumor cells. The second one exploited co-cultures of tumor cells and fibroblasts followed by cell sorting to isolate the fraction of individual fibroblasts. Human pancreatic cancer cells PANC-1 and MIA PaCa-2 as well as non-immortalized continuous fibroblasts from human skin were used in these experiments. Fibroblast activation was monitored using the fibroblast mRNA levels of the *ACTA2* gene expressing α-smooth muscle actin (α-SMA), *PDGFRA* expressing platelet-derived growth factor receptor-α (PDGFRα), and interleukin 6 (*IL-6*) by real-time PCR. In addition, the morphological character of activated fibroblasts was evaluated by the cell length-to-width ratio **[24,25].**

Fibroblast activation by conditioned media

Changes in cell morphological features: Analysis of fibroblast morphological changes **(Figure 1a)** demonstrates that the cell length-to-width ratio reaches ~10 one day after inoculation in the fresh medium or that conditioned by similar fibroblasts and does not significantly change during subsequent culture.

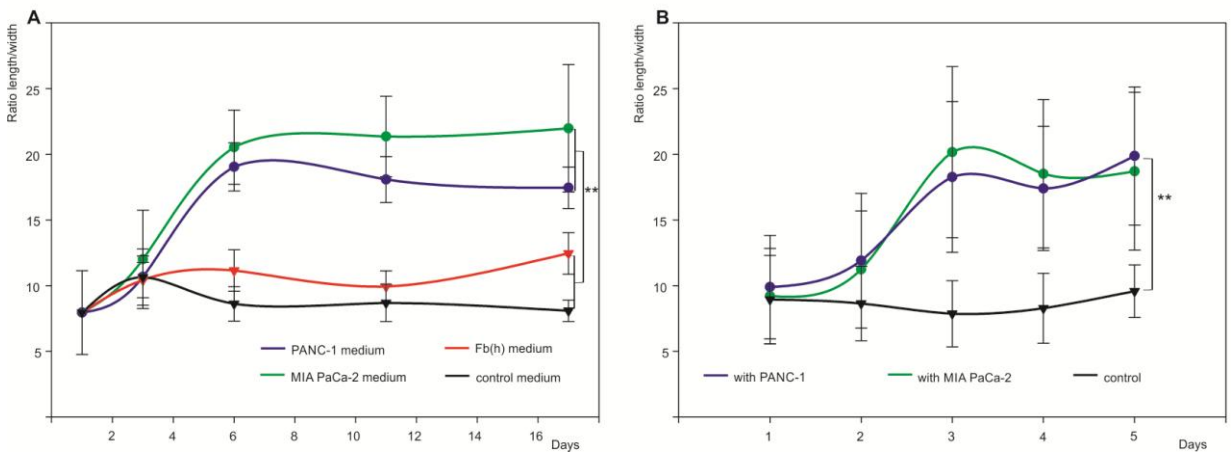

Figure 1: Dynamics of morphological parameters of human dermal fibroblasts Fb(h) grown in conditioned media (a) and co-cultured with cancer cells (b). Abscissa, time (days); ordinate, cell length-to-width ratio (mean ± SD, ** $p < 0.01$). The number of analyzed cells in each group was 60 - 90.

At the same time, exposure to medium conditioned by malignant PANC-1 and MIA PaCa-2 cells significantly modifies fibroblast morphology: the length-to-width ratio increases up to 20-fold six days after inoculation and remains steady by the end of the observation period **(Figure 2).**

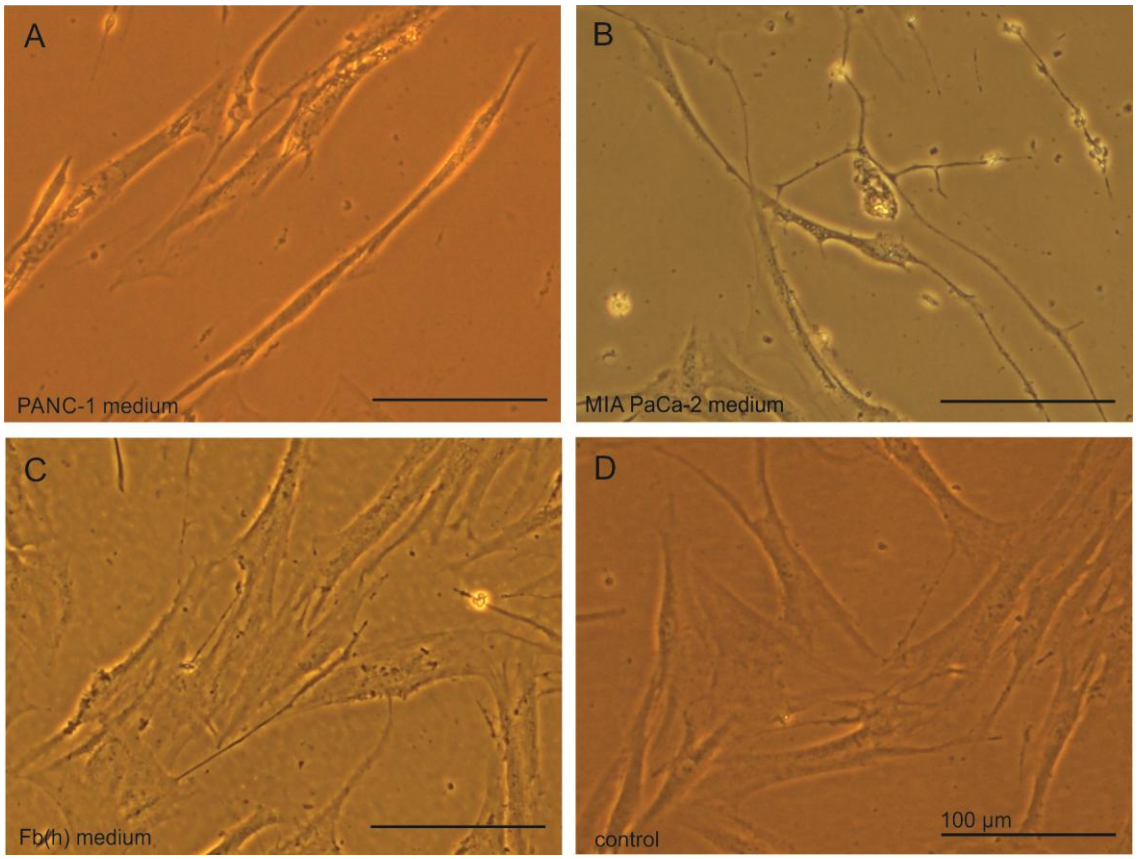

Figure 2: Morphology of Fb(h) during cultivation on conditioned media. Cell images obtained on day 12 of cultivation. (a, b, c) – Fb(h) in conditioned media obtained during the cultivation of PANC-1_GFP, MIA PaCa-2_GFP, Fb(h), respectively. (d) – Fb(h) in a standard media. Scale bar = 100 µm.

It should be noted that such elongation is not observed in all cells. About 30% of fibroblasts do not respond to the activation and maintain the initial length-to-width ratio. Thus, the morphological changes of the dermal primary fibroblasts growing in media conditioned by malignant PANC-1 or MIA PaCa-2 cells complete 6 days after the activation.

Changes in marker gene expression in fibroblast activation by conditioned media

Analysis of changes in the expression of selected marker genes by real-time PCR **(Figure 3a)** demonstrated decreased *IL-6* gene expression in fibroblasts only after extended incubation (15-20 days) in media conditioned by malignant PANC-1 and MIA PaCa-2 cells relative to control grown in fresh medium or that conditioned by the same fibroblasts. No significant differences in *PDGRFA* and *ACTA2* expression were observed in fibroblasts cultured on media conditioned by malignant cells relative to control **(Figure 3b and c).**

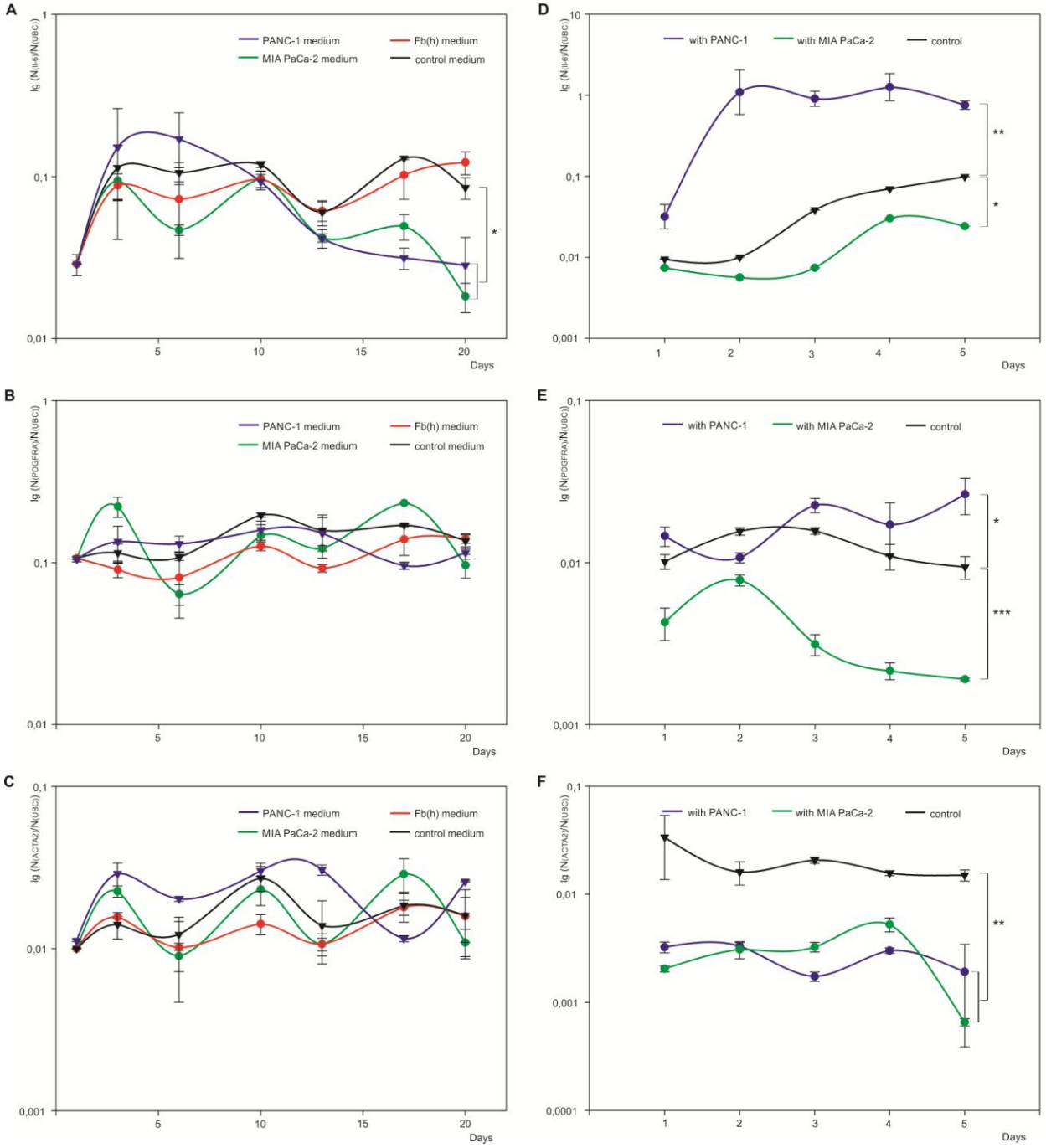

Figure 3: Expression dynamics of marker genes in Fb(h) cells grown in conditioned media (left) and co-cultured with cancer cells (right). (a-c), expression of marker genes *IL-6*, *PDGFRA*, *ACTA2*, respectively, in Fb(h) grown on conditioned media; (d-f), expression of marker genes *IL-6*, *PDGFRA*, *ACTA2*, respectively, in Fb(h) during co-cultured with cancer cells. Abscissa, time (days); ordinate, logarithm of the ratio between the initial expression levels of *IL-6*, *PDGFRA*, or *ACTA2* and reference *UBC* genes, ($N_{(GENE)}/N_{(UBC)}$). Data are presented as mean ± SD. * $p < 0.05$; ** $p < 0.01$; *** $p < 0.001$.

Thus, this activation method reveals no correlation between the fibroblast morphological characters and the expression levels of the marker genes studied. The data obtained suggest that the morphological changes in fibroblasts can be induced by paracrine factors released by cancer cells and are likely realized by molecular

mechanisms not directly related to the genetic networks involving the studied marker genes including *ACTA2*, whose product α-SMA is a cytoskeleton component.

Changes in migration potential of fibroblasts in vitro

The capacity of cells for migration is one of key properties for their involvement in the metastatic cascade. The fibroblast migration potential *in vitro* was evaluated using a Transwell system. The fibroblast migration rate to media conditioned by cancer cells was quantified against fresh medium as well as that conditioned by the same fibroblasts. The migration efficiency was evaluated after 24 and 48 h of culture. Figure 4 demonstrates equal efficiency of fibroblast migration to the fresh and fibroblast-conditioned media. In both cases, about 3% of cells migrated on days 1 and 2 of culture.

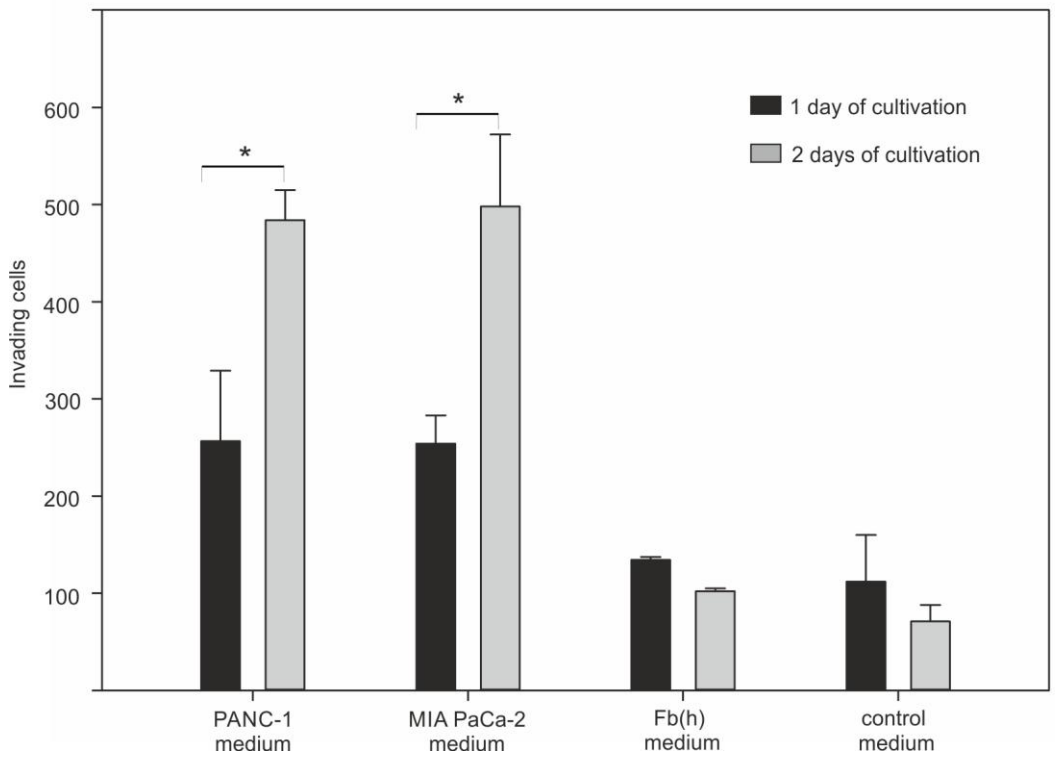

Figure 4: Migration activity of Fb(h)_CM DiI cells in Transwell system. The mean number of invasive cells on a Transwell membrane for three independent experiments ± SD is given. * $p < 0.05$.

In the case of media conditioned by both cancer cell lines, the migration efficiency reached 7.5 and 15% after 24 and 48 h of culture, respectively. Thus, paracrine factors released by cancer cells can rapidly promote fibroblast migration *in vitro*.

Activation of co-cultured fibroblasts

Changes in cell morphological status: Generally, morphological alterations of fibroblasts co-cultured with PANC-1 and MIA PaCa-2 cells were similar to those observed with media conditioned by cancer cells **(Figure 1a and b).** The length-to-width ratio increased in fibroblasts co-cultured with cancer cells from 10 to 20 and remained steady later. However, the morphological modifications proceeded faster and were completed after three days of culture **(Figure 5).** Thus, cell-to-cell interactions can further contribute to morphological changes of fibroblasts. This can be due to the higher efficiency of paracrine factors in close proximity between a cancer

cell and target fibroblast or cell-to-cell interactions implicate extra mechanisms to the induction of morphological changes.

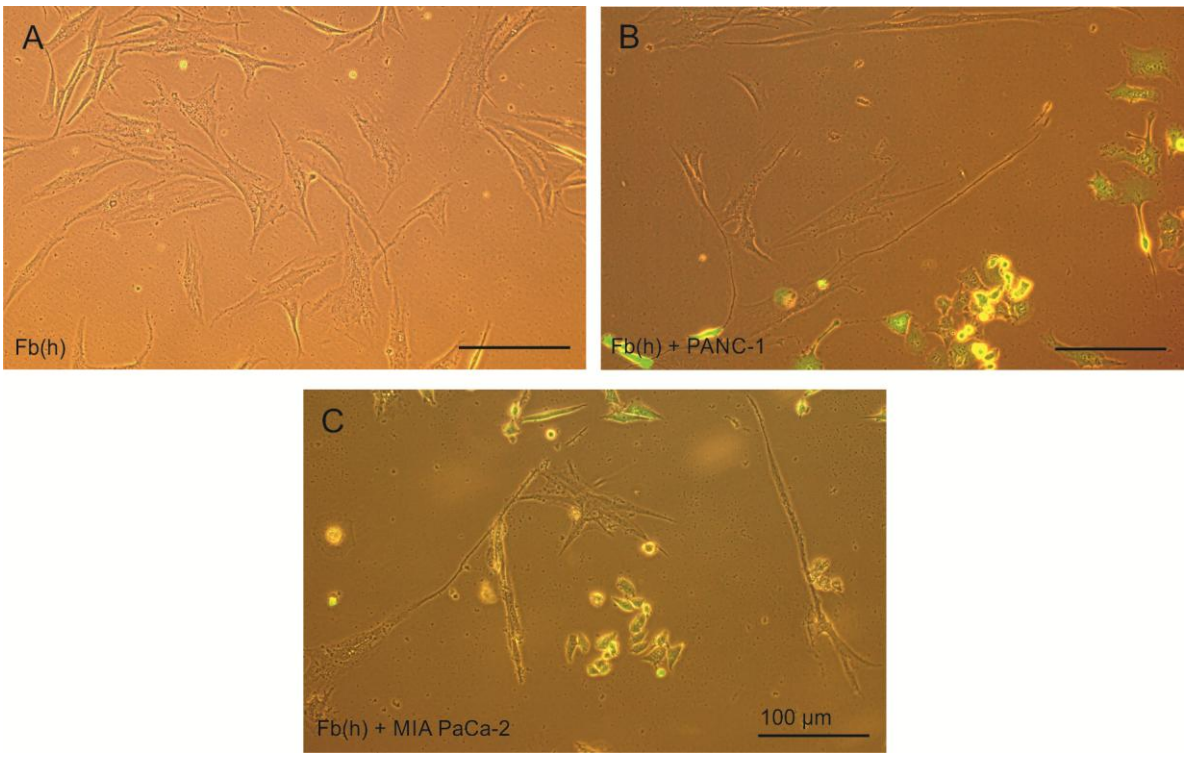

Figure 5: Morphology of Fb(h) during co-cultivation with PANC-1_GFP and MIA PaCa-2_GFP. Cell images obtained on the 3rd day of cultivation. (a) – Fb(h) in a standard media. (b, c) – Fb(h) co-cultivated with PANC-1_GFP, MIA PaCa-2_GFP, respectively, images obtained by overlaying fluorescent and visible images. Scale bar = 100 µm.

Notice that the elongation was not observed in all cells in co-culture as well. About 30% of fibroblasts were insensitive to the activation and preserved the initial length-to-width ratio.

Changes in marker gene expression in co-cultured fibroblasts

The changes in the marker gene expression in activated fibroblasts co-cultured with cancer cells differed for PANC-1 and MIA PaCa-2 cells as well as from the changes induced by conditioned media **(Figure 2d-f).** A significant increase in *IL-6* gene expression is observed in fibroblasts 48 h after co-culturing with PANC-1 but not MIA PaCa-2 cells. At the same time, decreased *ACTA2* expression is observed after 24 h of co-culture with both cancer cell lines, which is a marker of CAF activation **[26].** Thus, direct interaction with cancer cells rapidly modulates the expression of marker genes in fibroblasts, which is not observed in paracrine activation.

Evaluation of migration capacity of fibroblasts and cancer cells in vivo

The effect of co-culture with PANC-1 and MIA PaCa-2 cells on the functional state of fibroblasts as well as their migration potential and ability to modulate migration of cancer cells *in vivo* was assessed using an *in vivo* transplantation model in developing *Danio rerio*. Fibroblasts labeled with CM DiI were co-incubated with GFP-expressing PANC-1 or MIA PaCa-2 cells for 96 h and the cell suspension was transplanted into the yolk sac of *Danio rerio* 48 h after fertilization. The migration activity of fibroblasts and cancer cells was evaluated by

fluorescent microscopy 48 h after transplantation by counting embryos were transplanted cells migrated from the injection area **(Figure 6).**

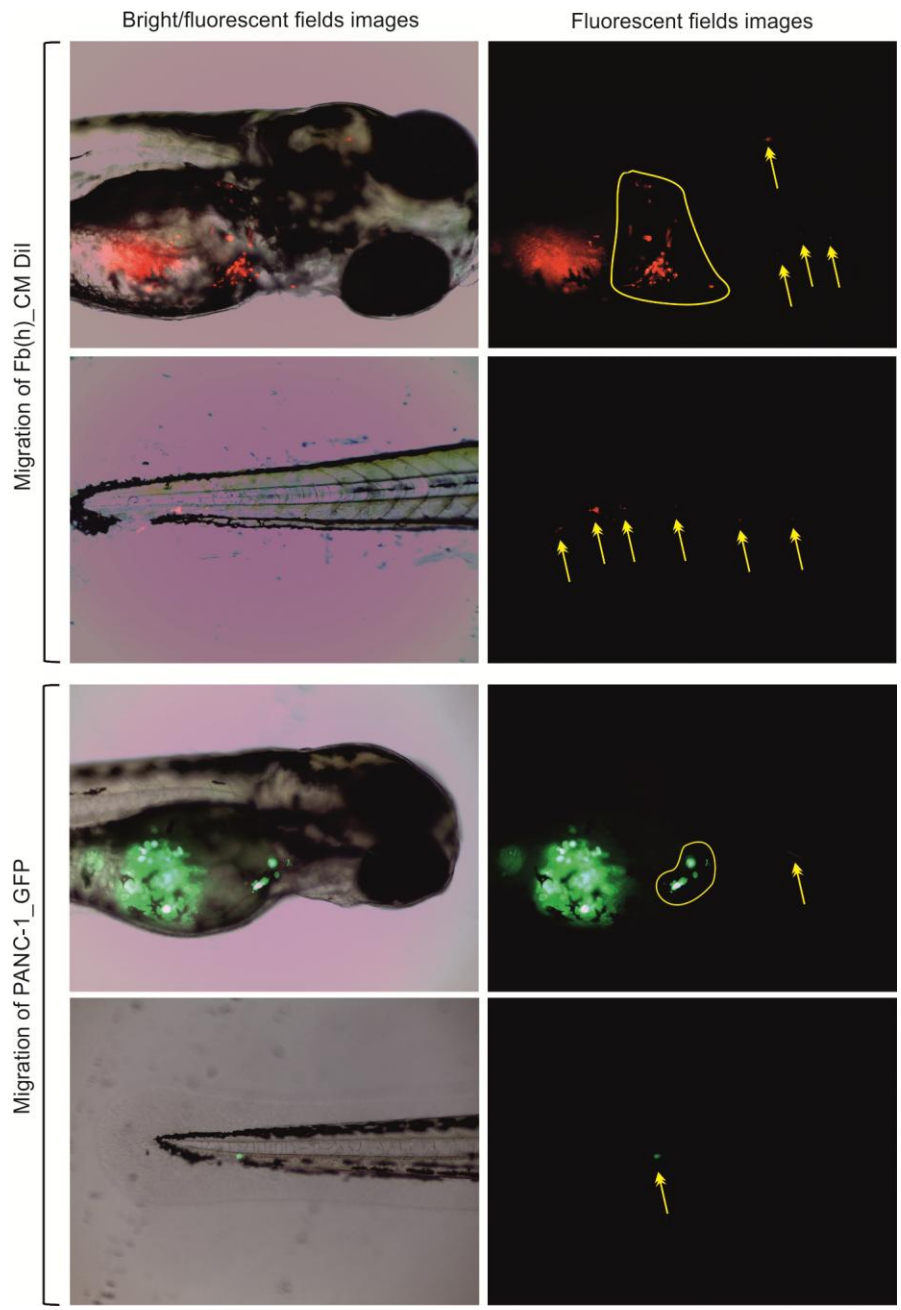

Figure 6: Migration activity of Fb(h)_CM DiI cells and cancer PANC-1_GFP cells in developing zebrafish embryo. Marked areas cover cells migrated to the perivitelline space from the injection site in the embryo. Arrows indicate cells migrated to cephalic or tail blood vessels. The image presents an embryo 48 hours post-transplantation. Magnification × 20.

Control experiments demonstrated cell migration from the injection area in 10, 10, and 2% embryos transplanted with individual cell cultures of fibroblasts, PANC-1, and MIA PaCa-2, respectively. In this case, mixing fibroblasts with cancer cells immediately before injection to zebrafish embryos or their co-culturing before

injection had no significant effect on the migration activity of either PANC-1 and MIA PaCa-2 cells or fibroblasts **(Figure 7).**

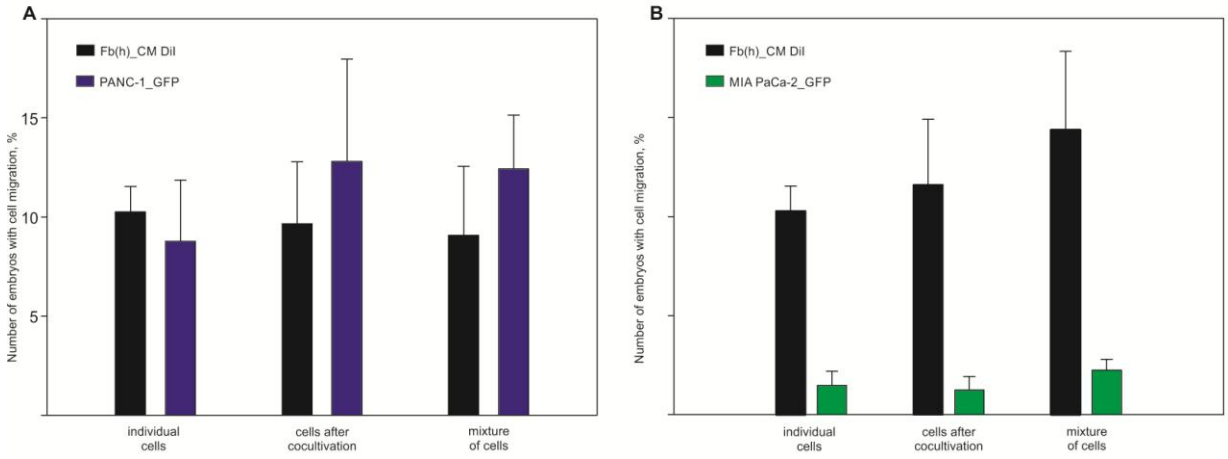

Figure 7: Comparison of migration activities of Fb(h)_CM DiI and cancer PANC-1_GFP (a) or MIA PaCa-2_GFP (b) cells after transplantation into the developing zebrafish embryo. Data averaged for two independent experiments are given. Cell suspensions of individual Fb(h)_CM DiI, PANC-1_GFP, and MIA PaCa-2_GFP cells; co-cultured Fb(h)_CM DiI/PANC-1_GFP and Fb(h)_CM DiI/MIA PaCa-2_GFP cells; as well as Fb(h)_CM DiI+PANC-1_GFP and Fb(h)_CM DiI+MIA PaCa-2_GFP cell suspensions mixed immediately prior to transplantation were used to inject 100 embryos each.

Discussion

Current published data allow us to state that CAFs mediate nearly all elements of the metastatic cascade from metabolic reprogramming, maintenance of tumor stemness, and collective invasion of tumor cells into the bloodstream within heterotypic clusters, to metastatic niche formation and angiogenesis of secondary tumor nodules **[27-29].** Thus, CAF-mediated metastasis can be a model covering different aspects of cell population migrations in the body. The identification of specific mechanisms underlying CAFs function can provide the basis for therapeutic "anti-stromal" approaches to metastasis suppression. It should be noted that, despite numerous data on the possible involvement of specific factors in CAFs formation, the fundamental pathways of fibroblast activation remain obscure, are complex, and, most importantly, the mechanisms of CAFs formation vary with tumors of different etiology. Published data demonstrate that CAFs are a mixture of cell subpopulations of different origin **[30-34].** Intratumor CAFs can be divided into several subtypes by the associated biological markers that demonstrate different expression patterns in cell subpopulations. At the same time, the expression of markers known to date is not limited to CAFs and neither of them is expressed in all CAFs subpopulations. Overall, the methods for reliable identification and classification of CAFs subtypes are underdeveloped and limited. Notice that the direction of changes in the level of the same markers can vary for individual CAF-tumor combinations including individual intratumor subpopulations of CAFs **[26].** Thus, the profile of the markers rather than the direction and level of changes in their expression is the hallmark of fibroblast activation. Here, we studied the changes in the expression of three marker genes, *ACTA2*, *PDGFRA*,

and *IL-6*, associated with CAFs formation and likely related to the regulation of various biochemical cascades involved in the process **[35-39].**

α-Smooth muscle actin (α-SMA), the product of the *ACTA2* gene, belongs to the actin family, a highly conserved group of proteins critical for the mobility and structural integrity of cells, and is the most common marker for activated fibroblasts **[26,30,33].** PDGFRα is a receptor of tyrosine kinases at the surface of fibroblasts, astrocytes, neural precursors, and pericytes **[40].** This is a common general marker for fibroblasts, and its expression in cancer-associated fibroblasts changes in patients with glioma, prostate and ovarian cancer, etc. **[38,39,41,42].** IL-6 is an anti-inflammatory cytokine whose expression increases in activated fibroblasts; in particular, this promotes the formation of pre-metastatic niches and enhances metastatic efficiency **[43-46].** The data obtained indicate several stages of changes in the functional state of fibroblasts induced by cancer cells, which are mediated by different mechanisms and aimed at different biological endpoints. The rapid increase in migration activity of fibroblasts exposed to media conditioned by cancer cells observed *in vitro* in a Transwell system suggests the recruitment of stromal fibroblasts to developing cancer induced by paracrine factors released by cancer cells at an early activation stage. Interestingly, the morphological state change of fibroblasts after paracrine activation is observed significantly later than their migration induction and is most pronounced after co-culture with cancer cells. Thus, the rearrangement of cell morphology is likely induced after stromal fibroblasts approach the tumor and can be aimed at a different biological function. Presumably, this stage of the process can activate fibroblasts for the recovery of damaged connective tissue and anticancer response. The observed paracrine activation does not directly engage the molecular mechanisms involving genetic networks of the used marker genes since the *PDGRFA* and *ACTA2* expression remains unaltered and *IL-6* expression decreases at the very late culture stages. At the same time, direct contact of fibroblasts with cancer cells rapidly induces changes in their morphological state and expression of marker genes. Thus, cell interaction with cancer cells involves extra molecular mechanisms into the activation that are not induced by paracrine exposure. Their co-culturing with PANC-1 cells increased *IL-6* expression combined and decreased *ACTA2* expression, which is typical of the inflammatory subtype of CAFs **[26].**

Notice that the decreased *ACTA2* expression in CAFs is also typical of many natural and experimental tumors. For instance, a significant decrease in *ACTA2* expression is observed in human fibroblasts co-cultured with organoids derived from pancreatic ductal adenocarcinoma patients **[26].** Such data are commonly interpreted as an indication of the inflammatory CAFs subtype formation. At the same time, fibroblast co-culturing with MIA PaCa-2 cells decreased *ACTA2* expression without increasing that of *IL-6*. This can indicate the formation of different CAFs subtypes under the influence of cancer cell lines used. Since the expression product of the *ACTA2* gene is a component of the cytoskeleton, which suggests that the observed morphological changes in the activated fibroblasts can be due to altered αSMA synthesis. Fibroblasts co-cultured with PANC-1 and MIA PaCa-2 cells demonstrated a decreased *ACTA2* expression. However, their activation after the exposure to media conditioned by these cancer cell cultures occurs without the suppression of *ACTA2* expression. Thus, the observed morphological changes in activated fibroblasts appear not to be directly related to the *ACTA2* expression level and its decreased expression when co-cultured with tumor cells can be targeted to a different biological function. Despite the activation characters such as morphological state and expression of CAF-associated markers, fibroblasts co-cultured with PANC-1 and MIA PaCa-2 cells failed to modulate the migration efficiency of cancer cells in the *in vivo* transplantation model with zebrafish embryos. The acquired

capacity for CAF-dependent transport of cancer cells can be due to the involvement of additional activation mechanisms possibly targeted at specific CAFs subpopulations. Developing tumor is a changing population of highly genetically and epigenetically heterogeneous cells that can acquire various functional properties; however, there are limits to their evolutionary opportunities. Cancer cannot go beyond the body, which renders the long-term evolution of cancer cells impossible, it is limited to the body and its lifespan. Nevertheless, cancer makes use of highly complex biological mechanisms. However, this discussion should focus on the migration of cancer cells. According to recent studies, metastasis is not independently realized by cancer cells. Their migration, overcoming tissue barriers, efficient inter- and extravasation, and formation of secondary tumor nodules require a complex tumor interaction with the surrounding stromal tissue **[1,3,4].** It seems unlikely that the processes controlling the function of normal cells can emerge *de novo* as individual cancer progresses. Their pre-existence is more likely, which assumes a specific function of such processes. Accordingly, developing tumor presumably utilizes processes intended for different purposes. Dissemination of individual cell populations in embryonic development is the most likely initial mechanism of indirect transfer of cancer cells. In this case, the ability to mimic normal cells requesting migration acquired by certain cancer cells could trigger metastasis.

Acknowledgments

In vivo experiments were carried out on the equipment of the Center for Collective Use of the Institute of Molecular Genetics of National Research Centre “Kurchatov Institute”.

This work was supported in part by the Kurchatov Genomic Center Development Program (Grant Number 075-15-2019-1664), in part by Russian Ministry of Science and Higher Education (Grant Number 075-15-2021-1062).

Declarations

Ethics approval and informed consent

Experiments on animals were conducted in strict accordance with the ethics principles prescribed by the European Convention for the Protection of Vertebrates and the bioethics norms (https://rm.coe.int/168007a67b). This study was performed in line with the principles of the Declaration of Helsinki. Approval was granted by the Ethics Committee of the Institute of Molecular Genetics of National Research Centre “Kurchatov Institute” (protocol # 1, 11 January 2022).

Data availability

The data presented in this study are available on request from the corresponding author.

Competing interests

The author reports no conflicts of interest in this work.

Authors' contributions

Conceptualization: Sergey Kostrov and Dina Safina; methodology: Dina Safina, Nataliya Lunina, Marina Roschina, Sergey Kostrov; investigation: Dina Safina, Nataliya Lunina, Marina Roschina, Oksana Staeglasova, Andrey Kazakov; data curation: Dina Safina, Nataliya Lunina; writing—original draft preparation: Dina Safina, Sergey Kostrov; writing—review and editing: Dina Safina, Nataliya Lunina, Vladimir Demkin, Ilya Demidyuk,

Sergey Kostrov; supervision, Sergey Kostrov; funding acquisition: Ilya Demidyuk, Sergey Kostrov. All authors have read and agreed to the published version of the manuscript.

References

1. Hinshaw DC, Shevde LA. The tumor microenvironment innately modulates cancer progression. Cancer. Res. 2019;79(18):4557-66.
2. Kong J, Tian H, Zhang F, Zhang Z, Li J, Liu X, et al. Extracellular vesicles of carcinoma-associated fibroblasts creates a pre-metastatic niche in the lung through activating fibroblasts. Mol Cancer. 2019;18(1):175.
3. Koustoulidou S, Hoorens MWH, Dalm SU, Mahajan S, Debets R, Seimbille Y, et al. Cancer-associated fibroblasts as players in cancer development and progression and their role in targeted radionuclide imaging and therapy. Cancers (Basel). 2021;13(5):1100.
4. Kwa MQ, Herum KM, Brakebusch C. Cancer-associated fibroblasts: How do they contribute to metastasis? Clin Exp Metastasis. 2019;36(2):71-86.
5. Joshi RS, Kanugula SS, Sudhir S, Pereira MP, Jain S, Aghi MK. The role of cancer-associated fibroblasts in tumor progression. Cancers (Basel). 2021;13(6):1399.
6. Kim J, Hong SJ, Park JY, Park JH, Yu YS, Park SY, et al. Epithelial-mesenchymal transition gene signature to predict clinical outcome of hepatocellular carcinoma. Cancer Sci. 2010;101(6):1521-28.
7. Ye X, Weinberg RA. Epithelial-mesenchymal plasticity: a central regulator of cancer progression. Trends Cell Biol. 2015;25(11):675-86.
8. Matsumura Y, Ito Y, Mezawa Y, Sulidan K, Daigo Y, Hiraga T, et al. Stromal fibroblasts induce metastatic tumor cell clusters via epithelial–mesenchymal plasticity. Life Sci Alliance. 2019;2(4):e201900425.
9. Li J, Jia Z, Kong J, Zhang F, Fang S, Li X, et al. Carcinoma-associated fibroblasts lead the invasion of salivary gland adenoid cystic carcinoma cells by creating an invasive track. PLoS One. 2016;11(3):1-15.
10. Ortiz-Otero N, Clinch AB, Hope J, Wang W, Reinhart-King CA, King MR. Cancer associated fibroblasts confer shear resistance to circulating tumor cells during prostate cancer metastatic progression. Oncotarget. 2020;11(12):1037-50.
11. Burr R, Gilles C, Thompson EW, Maheswaran S. Epithelial-mesenchymal plasticity in circulating tumor cells, the precursors of metastasis. Adv Exp Med Biol. 2020;1220:11-34.
12. DePalma M, Biziato D, Petrova TV. Microenvironmental regulation of tumour angiogenesis. Nat Rev Cancer. 2017;17(8):457-74.
13. Monteran L, Erez N. The dark side of fibroblasts: cancer-associated fibroblastsas mediators of immunosuppression in the tumor microenvironment. Front Immunol. 2019;10:1835.
14. Prieto-García E, Díaz-García CV, Agudo-López A, Pardo-Marqués V, García-Consuegra I, Asensio-Peña S, et al. Tumor–stromal interactions in a co-culture model of human pancreatic adenocarcinoma cells and fibroblasts and their connection with tumor spread. Biomedicines. 2021;9(4):364.
15. Valkenburg KC, de Groot AE, Pienta KJ. Targeting the tumour stroma to improve cancer therapy. Nat Rev Clin Oncol. 2018;15(6):366-81.

16. Walter SG, Scheidt S, Nibler R, Gaisendrees C, Zarghooni K, Schildberg FA. In-depth characterization of stromal cells within the tumor microenvironment yields novel therapeutic targets. Cancers. 2021;13(6):1466.
17. Chen X, Song E. Turning foes to friends: targeting cancer-associated fibroblasts. Nat Rev Drug Discov. 2019;18(2):99-115.
18. Shah K, Mallik SB, Gupta P, Iyer A. Targeting tumour associated fibroblasts in cancers. Front Oncol. 2022;12:908156.
19. Olson HM, Nechiporuk AV. Using zebrafish to study collective cell migration in development and disease. Front Cell Dev Biol. 2018;6:83.
20. Stuelten CH, Parent CA, Montell DJ. Cell motility in cancer invasion and metastasis: insights from simple model organisms. Nat Rev Cancer. 2018;18(5):296-312.
21. Alieva AKh, Rudenok MM, Novosadova EV, Vlasov IN, Arsenyeva EL, Rosinskaya AV, et al. Whole-transcriptome analysis of dermal fibroblasts, derived from three pairs of monozygotic twins, discordant for Parkinson's disease. J Mol Neurosci. 2020;70(2):284-93.
22. Kondratyeva LG, Safina DR, Chernov IP, Kopantzev EP, Kostrov SV, Sverdlov ED. PDX1, a key factor in pancreatic embryogenesis, can exhibit antimetastatic activity in pancreatic ductal adenocarcinoma. Cancer Manag Res. 2019;11:7077-87.
23. Kubista M, Andrade JM, Bengtsson M, Forootan A, Jonák J, Lind K, et al. The real-time polymerase chain reaction. Mol Aspects Med. 2006;27(2-3):95-125.
24. Bolm L, Cigolla S, Wittel UA, Hopt UT, Keck T, Rades D, et al. The role of fibroblasts in pancreatic cancer: extracellular matrix versus paracrine factors. Transl Oncol. 2017;10(4):578-88.
25. Kondratyeva L, Chernov I, Kopantzev E, Didych D, Kuzmich A, Alekseenko I, et al. Pancreatic Lineage Specifier PDX1 Increases Adhesion and Decreases Motility of Cancer Cells. Cancers (Basel). 2021;13(17):4390.
26. Öhlund D, Handly-Santana A, Biffi G, Elyada E, Almeida AS, Ponz-Sarvise M, et al. Distinct populations of inflammatory fibroblasts and myofibroblasts in pancreatic cancer. J Exp Med. 2017;214(3):579-96.
27. Zhou Q, Wu X, Wang X, Yu Z, Pan T, Li Z, et al. The reciprocal interaction between tumor cells and activated fibroblasts mediated by TNF-α/IL-33/ST2L signaling promotes gastric cancer metastasis. Oncogene. 2019;39(7):1414-28.
28. Zhang DX, Vu LT, Ismail NN, Le MTN, Grimson A. Landscape of extracellular vesicles in the tumour microenvironment: Interactions with stromal cells and with non-cell components, and impacts on metabolic reprogramming, horizontal transfer of neoplastic traits, and the emergence of therapeutic resistance. Semin Cancer Biol. 2021;74:24-44.
29. Hurtado P. Martínez-Pena I, Piñeiro R. Dangerous liaisons: circulating tumor cells (CTCs) and cancer-associated fibroblasts (CAFs). Cancers (Basel). 2020;12(10):2861-84.
30. Kalluri R. The biology and function of fibroblasts in cancer. Nat Rev Cancer. 2016;16(9):582-98.
31. Bartoschek M, Oskolkov N, Bocc M, Lövrot J, Larsson C, Sommarin M, et al. Spatially and functionally distinct subclasses of breast cancer associated fibroblasts revealed by single cell RNA sequencing. Nat Commun. 2018;9(1):5150.

32. Neuzillet C, Tijeras-Raballand A, Ragulan C, Cros J, Patil Y, Martinet M, et al. Inter- and intra-tumoural heterogeneity in cancer-associated fibroblasts of human pancreatic ductal adenocarcinoma. J Pathol. 2019;248(1):51-65.
33. Sahai E, Astsaturov I, Cukierman E, DeNardo DG, Egeblad M, Evans RM, et al. A framework for advancing our understanding of cancer-associated fibroblasts. Nat Rev Cancer. 2020;20(3):174-86.
34. Boyd LNC, Andini KD, Peters GJ, Kazemier G, Giovannetti E. Heterogeneity and plasticity of cancer-associated fibroblasts in the pancreatic tumor microenvironment. Semin Cancer Biol. 2022;82:184-96.
35. Ozdemir BC, Pentcheva-Hoang T, Carstens JL, Zheng X, Wu CC, Simpson TR, et al. Depletion of carcinoma-associated fibroblasts and fibrosis induces immunosuppression and accelerates pancreas cancer with reduced survival. Cancer Cell. 2014;25(6):719-34.
36. Mezawa Y, Orimo A. The roles of tumor- and metastasis-promoting carcinoma-associated fibroblasts in human carcinomas. Cell Tissue Res. 2016;365(3):675-89.
37. Costa A, Kieffer Y, Scholer-Dahirel A, Pelon F, Bourachot B, Cardon M, et al. Fibroblast heterogeneity and immunosuppressive environment in human breast cancer. Cancer Cell. 2018;33(3):463-79.
38. Strell C, Paulsson J, Jin SB, Tobin NP, Mezheyeuski A, Roswall P, et al. Impact of Epithelial-Stromal interactions on peritumoral fibroblasts in ductal carcinoma *in situ*. J Natl Cancer Inst. 2019;111(9):983-95.
39. Nurmik M, Ullmann P, Rodriguez F, Haan S, Letellier E. In search of definitions: cancer-associated fibroblasts and their markers. Int J Cancer. 2020;146(4):895-905.
40. Funa K, Sasahara M. The roles of PDGF in development and during neurogenesis in the normal and diseased nervous system. J Neuroimmune Pharmacol. 2013;9(2):168-81.
41. Heldin C-H. Targeting the PDGF signaling pathway in tumor treatment. Cell Commun Signal. 2013;11:97.
42. Farahani RM, Xaymardan M. Platelet-derived growth factor receptor alpha as a marker of mesenchymal stem cells in development and stem cell biology. Stem Cells Int. 2015;2015:362753.
43. Wu X, Tao P, Zhou Q, Li J, Yu Z, Wang X, et al. IL-6 secreted by cancer-associated fibroblasts promotes epithelial-mesenchymal transition and metastasis of gastric cancer via JAK2/STAT3 signaling pathway. Oncotarget. 2017;8:20741-50.
44. Liu Q, Liao Q, Zhao Y. Chemotherapy and tumor microenvironment of pancreatic cancer. Cancer Cell Int. 2017;17:68.
45. Goulet CR, Champagne A, Bernard G, Vandal D, Chabaud S, Pouliot F, et al. Cancer-associated fibroblasts induce epithelial–mesenchymal transition of bladder cancer cells through paracrine IL-6 signaling. BMC Cancer. 2019;19(1):1-13.
46. Ji Q, Zhou L, Sui H, Yang L, Wu X, Song Q, et al. Primary tumors release ITGBL1-rich extracellular vesicles to promote distal metastatic tumor growth through fibroblast-niche formation. Nat Commun. 2020;11:1211.

Citation of this Article

Safina D, Lunina N, Roschina M, Staeglasova O, Kazakov A, Demkin V, Demidyuk I and Kostrov S. Activation of Human Fibroblasts by Pancreatic Cancer Cell Lines. Mega J Case Rep. 2023; 6: 2001-2016.

Copyright